

Quantum size and surface effects in the electrical resistivity and high-energy electron reflectivity of ultrathin lead films

M. Jałochowski

Institute of Physics, Department of Experimental Physics, University of Marie Curie-Skłodowska, place Marie Curie-Skłodowskiej 1, PL-20-031 Lublin, Poland

E. Bauer

Physikalisches Institut, Technische Universität Clausthal, D-3392 Clausthal-Zellerfeld, Federal Republic of Germany
(Received 16 February 1988; revised manuscript received 2 May 1988)

Oscillations of the electrical resistivity of thin epitaxial Pb films on Si(111) surfaces and of the intensity of the specular beam in high-energy electron diffraction from these films are reported. They are in part due to a surface effect, the scattering of internal and external electrons at surface steps whose density varies periodically during the growth. In part they are caused by a volume effect, the quantum size effect due to the quantization of the Fermi momentum of the film electrons and of the normal component of the wave vector of the incident electrons, respectively.

I. INTRODUCTION

When the dimension of a solid becomes very small in one direction, say the z direction, then the component of the wave vector of electrons in this direction, k_z , becomes quantized. This leads to the so-called quantum size effects (QSE) which have been theoretically predicted and in part also observed in many phenomena involving electrons in thin metal films. These phenomena may be divided in two groups: those involving the conduction electrons in the solid and those involving electrons injected into the solid from the outside. In the first group the QSE causes oscillatory variations of the Fermi energy E_F , of the electron density at E_F , of the work function, of the electrical resistivity, and of other quantities with film thickness. A large amount of theoretical work has been done on this subject (for references see Refs. 1–4) but little convincing experimental evidence of these QSE's is available for metals. Clear evidence of the QSE comes from the second group: (i) the fundamental electron tunneling experiments of Jaklevic *et al.*⁵ into thin (111) oriented Pb, Ag, Au, and (0001)-oriented Mg films and subsequent experiments of this type, and (ii) the low-energy electron transmission experiments of Jonker *et al.*⁶ through thin Cu and Ag films on W(110), thin Ag films on Cu(111), and thin Cu films on Ni(100).

The reason for the elusiveness of the QSE is the difficulty of preparing sufficiently thin metal films which are bounded by parallel surfaces. Much of the success of a QSE experiment depends, therefore, on the preparation technique of the films. Jaklevic *et al.*⁵ succeeded by making use of the tendency of metals to form a texture with the most closely packed plane parallel to the substrate when deposited in very thin films at low temperatures and annealed. Their substrate was a gas discharge anodized Al layer on glazed ceramic. Jonker *et al.*⁶ made use of the fact that metals with low surface energy grow on high surface energy metals in a monolayer-by-

monolayer mode⁷ ("Frank–van der Merwe mode") which has been clearly demonstrated for the first five atomic layers by Auger electron spectroscopy⁸ and for thicker films more recently by reflection high-energy electron diffraction (RHEED).⁹

Unfortunately, metallic substrates exclude the measurement of the electrical resistivity of the films. For this purpose insulating or at least semi-insulating substrates have to be used. On insulating substrates metals grow as a rule via formation of isolated three-dimensional nuclei ("Volmer-Weber mode"⁷). The film becomes continuous only after a critical thickness has been reached which depends upon metal, substrate, and deposition conditions. Unless deposited under conditions which lead to a good equilibrium plane texture the films are fine crystalline and so rough that diffuse reflection of the electrons at the film boundaries and thickness variations suppress the QSE. In a comparative electron tunneling and electrical resistivity study of quasicrystalline Pt films (grain size < 2 nm) on glass Fischer *et al.*¹⁰ found that the experimental conditions for the observability of the QSE of the electrical resistivity were much more stringent than those needed to see the QSE in electron tunneling. The complicated band structure of Pt and the imperfect structure of the films made an analysis of the data difficult but nevertheless they could be fitted satisfactorily by superposition of two oscillations, one due to electrons with a Fermi wavelength $\lambda_F = 0.26$ nm and one due to holes with $\lambda_F = 0.8$ nm. QSE experiments with other metals failed because of too large roughness of the film surface.¹⁰

We have recently succeeded¹¹ in growing Ag and Au single-crystal films on a semi-insulating substrate, Si(111), in quasi-monolayer-by-monolayer fashion as evidenced by RHEED specular beam intensity oscillations and have measured the electrical resistivity of the growing films. Clear resistivity oscillations were observed; however, they were not related to λ_F but could be attributed to periodic changes of the specularity parameter p due to periodic

variation of the density of surface scattering centers (monoatomic steps) with increasing thickness. As these Ag and Au films are much more perfect than the previously studied Pt films¹⁰ the existence of QSE resistivity oscillations in these Pt films appears questionable. In the present paper we report oscillations which are clearly linked to λ_F of a metal with a much simpler band structure, Pb, which demonstrate the QSE of the electrical resistivity unambiguously. In the same films, oscillations in the RHEED specular beam intensity are seen which are best pronounced when the normal component of the wave vector of the incident electrons fulfills the QSE condition $k_z = n\pi/d$ (n integer, d film thickness). Thus, the QSE effect is demonstrated simultaneously for internal and external electrons, differing in energy by many orders of magnitude.

II. THEORETICAL BACKGROUND

A. Electrical resistivity

The electrical resistivity ρ of a thin layer of thickness d is usually described by the theory of Fuchs¹² in terms of the bulk resistivity ρ_∞ , the mean free path of the conduction electrons l , and the specularly parameter p which is the fraction of electrons specularly reflected from the surfaces. The general expression of Fuchs is inconvenient for data analysis which is usually done in terms of the thick-film and the thin-film approximations of Sondheimer,¹³

$$\rho = \rho_\infty \left[1 + \frac{3}{8}(1-p)\frac{l}{d} \right] \quad (d \gg l) \quad (1)$$

and

$$\rho = \rho_\infty \frac{4}{3} \frac{1-p}{1+p} \frac{l}{d} \frac{1}{\ln(l/d)} \quad (d \ll l). \quad (2)$$

Equation (1) actually is a very good approximation down to $d/l \approx 0.1$, in particular for large p , while Eq. (2) is valid only for $d \ll l$ (Ref. 14) and small p .

Numerous generalizations of the Fuchs-Sondheimer formulas have been made taking into account the angular dependence of p , surface roughness, grain boundary scattering, and other factors (for references see Refs. 15–17). In view of the single crystalline structure and the planar boundaries of the layers used in our work, these extensions of the theory will not be discussed here. What has to be taken into account, however, is the possibility of different specularly parameters of the free surface and of the interface with the substrate,¹⁸ p and q . In this case, the asymptotic expressions are¹⁸

$$\rho = \rho_\infty \left[1 + \frac{3}{8} \left(1 - \frac{p+q}{2} \right) \frac{l}{d} \right] \quad (d \gg l) \quad (3)$$

and

$$\rho = \rho_\infty \frac{4}{3} \frac{1-pq}{(1+p)(1+q)} \frac{l}{d} \frac{1}{\ln(l/d)} \quad (d \ll l). \quad (4)$$

Comparison with Eqs. (1) and (2) shows that the parameter p in the Sondheimer expressions is an effective specu-

larity parameter given by $p_1 = (p+q)/2$ and $p_2 = (p+q)/2 - [(p-q)/2]^2 / [1 + (p+q)/2]$, respectively. Thus, when measurements of the specularly parameters p_1 and p_2 in the thick-film and very-thin-film limits, respectively, give different values then p and q must differ and can be calculated from p_1, p_2 :

$$(p, q) = p_1 \pm [(p_1 - p_2)(1 + p_1)]^{1/2}. \quad (5)$$

Such an analysis is, of course, only meaningful if the film has the same structure over the whole thickness range so that ρ_∞, l, p , and q are independent of d . To be more precise, the average values of p and q must be independent of d . As mentioned already earlier, we have shown recently that the effective specularly parameter changes periodically with d , which was attributed to the periodic variation of the density of surface steps in a monolayer-by-monolayer growth process.¹¹ These periodic variations of p_{eff} have to be attributed solely to the free surface, say p , because the specularly parameter of the interface, say q , should not change with d .

Superimposed on the ρ oscillations due to p oscillations are the QSE oscillations provided the QSE condition $k_z = n\pi/d$ is fulfilled for electrons at the Fermi surface, i.e., for $d = n\lambda_F/2$. As d can change only in multiples of the monolayer thickness d_0 and as d_0 and λ_F are in general incommensurate, the QSE condition is fulfilled only over limited thickness ranges $m_1 d_0 \leq d \leq m_2 d_0$ for which $md_0 \approx n\lambda_F/2$ ($m_1 \leq m \leq m_2$). The frequently used picture of regular sawtoothlike ρ oscillations which is based on a continuously changing film thickness is (see, e.g., Ref. 19), therefore, not very realistic. Rather, one has to expect thickness ranges with large QSE amplitudes separated by regions in which no QSE can be seen because of the d_0 - λ_F mismatch.

Lead was chosen in the present study because of its nearly-free-electron Fermi surface and its well-known electronic structure.^{20–22} The Fermi energy of bulk Pb is $E_F = 9.8$ eV and its effective mass in the [111] direction $m^* = 1.14m_0$ (Ref. 20) so that $\lambda_F = h/(2m^*E_F)^{1/2} = 0.366$ nm. The (111) monolayer thickness in the bulk is $d_0 = a/\sqrt{3} = 0.286$ nm. Thus we have $(\lambda_F/2):d_0 = 0.183:0.286 = 2:3.12 \approx 2:3$ and as a consequence the QSE condition $md_0 \approx n\lambda_F/2$ is only approximately fulfilled for $(m, n) = (2, 3)$ and $(4, 6)$ but no further matching occurs until about $(m, n) = (7, 11)$ and $(9, 14)$ with later matching regions centered around $(m, n) = (13, 20)$ and $(20, 31)$. Although the matching is much better at the larger (m, n) ratios the requirements for the flatness of the film are much more stringent at larger d . It must also be kept in mind that E_F and, therefore, λ_F depends upon film thickness, at least in the simple symmetric rectangular potential-well model of the film.⁴ d_0 may change, too, with d but to only a small extent. Thus the condition $md_0 \approx n\lambda_F/2$ with bulk d_0, λ_F values can only be a guideline in the search for the QSE in the resistivity.

Another limitation to the application of the theoretical models to films on substrates is the asymmetry in the experimental situation in contrast to the assumption of identical boundary planes in the models. How extreme this asymmetry is can be seen as follows. The potential

energy of an electron in a solid may be described by the energy of the bottom of the conduction or valence band with respect to the vacuum level. For Pb the values $V_0=16.6$ eV and $V_0=11.8+\phi=16.2$ eV have been calculated^{21,22} where a work function ϕ of the Pb(111) surface of 4.4 eV has been used. The experimental value is $V_0=10.5+4.4=14.9$ eV.²² For Si $V_0=W+E_\Gamma+\phi=17.6$ eV, where $W=12.4$ eV is the width of the valence band,²³ $E_\Gamma=0.4$ eV the energy of the top of the valence band with respect to E_F in pure Si, and $\phi=4.8$ eV the work function of the Si(111) plane.²⁴ Thus there is practically no confining potential wall at the Pb/Si interface (16.6 versus 17.6 eV) in the model of the potential well.

That the conduction electrons are confined to the film has a different reason: At the Pb/Si interface a Schottky barrier about 0.8 eV high is formed which keeps the electrons from entering the substrate. But even if there were no Schottky barrier, electrons at the Fermi level could not enter the semiconducting substrate because there are no propagating states at this energy to which the electron wave functions in the film could be matched, except under extreme degeneracy conditions. Possible interface states at E_F can act only as scattering centers because of their exponential decay into the substrate. These considerations show (i) that the conduction electrons are confined to the film and (ii) that the specular parameters of the two surfaces should differ considerably due to the completely different nature of the two boundaries.

B. RHEED specular beam intensity oscillations

The RHEED pattern of a flat single-crystal surface consists usually of streaks normal to the surface. Within the framework of the kinematic diffraction theory the intensity distribution along the streaks is determined by the distribution of atomic steps on the surface, provided the electron beam is sufficiently monochromatic and parallel, which is generally the case. Neglecting absorption and thermal diffuse scattering, the intensity along the streaks is concentrated into sharp spots when the coherently illuminated surface region is free of steps. In the other extreme case—a high concentration of steps, bounding small terraces of monoatomic height on various height levels which produce an undulating surface—the intensity is distributed evenly along the streaks. Typical monolayer-by-monolayer growth situations are in between these two extremes. The condensing atoms in part form two-dimensional islands, generating a new terrace (level), and in part are incorporated at steps, thus enlarging already existing islands. If only two levels are involved then the step density oscillates with the period of the deposition time of one monolayer. These oscillations are best seen in out-of-phase conditions, i.e., when the waves scattered from the two levels interfere destructively.

The resulting RHEED intensity oscillations which are most conveniently observed in the specular beam have been analyzed thoroughly within the framework of the kinematic diffraction theory²⁵ and the growth processes assumed in this analysis have been well documented by computer simulations.²⁶ The step density is determined

by the competition between island nucleation and island growth. These processes are controlled by the arrival rate r of the atoms and the rate of their incorporation into islands which depends via the rate of surface diffusion on the temperature. Therefore, only within a narrow (r, T) range can stable oscillations be maintained. If r is too low or T too high the step density becomes too low to be observable; if r is too high or T too low the oscillations die out rapidly due to increasing roughness of the surface. In the present study both conditions were met.

Superimposed on these oscillations which depend upon the surface perfection are the QSE oscillations which are connected with the thickness by the condition $k_z = n\pi/d$, provided of course that they can exist. This requires (i) that free surface and interface have sufficient specular reflectivity ($p, q > 0$), (ii) that the film has constant thickness over the distance necessary to set up the interference pattern between the reflected waves, and (iii) that inelastic scattering is sufficiently weak to maintain the coherence needed for interference. From the inner potential considerations in Sec. II A it appears as if the Pb/Si interface should have a negligible reflectivity. However, the effective inner potentials for fast electrons differ for the two materials, with $V_0=18.25-19.4$ eV for Pb and $V_0=11.5-12.2$ eV for Si.²⁷ In addition, for wave propagation from the Pb layer into the Si substrate it is also necessary that the wave functions must match at the interface. As the periodicity of the substrate is quite different from that of the layer no good matching is possible and the wave is at least partially reflected even in the absence of a significant potential step at the interface.

The limitations set by conditions (ii) and (iii) become less serious with increasing angle of incidence. If V_0 is the mean inner potential in the layer, E the kinetic energy of the electrons, and θ the glancing angle of incidence then the normal component of the wave vector in the film is given by

$$\begin{aligned} k_z &= k_0 \left[\frac{E + V_0}{E} \right]^{1/2} \left[1 - \frac{E}{E + V_0} \cos^2 \theta \right]^{1/2} \\ &= k_0 \left[\sin^2 \theta + \frac{V_0}{E} \right]^{1/2}. \end{aligned} \quad (6)$$

This k_z has to fulfill the QSE condition $k_z = n\pi/d$. In contrast to the electrical resistivity in which only electrons with fixed $k = k_F$ are available, k_z can be changed here by varying θ so that the conditions can be optimized.

III. EXPERIMENT

The experiments were performed in an ultrahigh-vacuum molecular beam epitaxy system which was equipped with a RHEED system. The base pressure was 8×10^{-11} mbar and the pressure during deposition was kept below 3×10^{-10} mbar. The substrates were Si(111) wafers with about $10 \Omega \text{ cm}$ resistivity at room temperature and typical dimensions $12 \times 3 \times 0.6$ mm. After chemical etching the final surface cleaning was performed in the vacuum system before deposition by flashing for a

few seconds to about 1550 K, which produced a clean Si(111) surface as indicated by a sharp Si(111)-(7×7) RHEED pattern²⁷ without SiC contamination. This type of surface is called type I in the following. Another type of surface (type II) was prepared by room-temperature deposition of one monolayer (ML) of Au on a type-I substrate, followed by annealing for 3 min at about 950 K and for 3 min at about 700 K. This type of surface showed a well-developed Au(6×6) RHEED pattern.²⁸

Direct resistive heating of the Si crystal was used. The holder could be rotated about the crystal normal so that any desired azimuth could be selected for the RHEED intensity measurements. The substrate could be cooled to about 95 K by making thermal contact between the rotatable holder and a liquid N₂ container.

Pb was evaporated from a BN crucible, Au from a W basket. The evaporators were surrounded by a liquid-N₂-cooled cold wall. Deposition rates between 0.05 and 0.1 nm/s were used for Pb; for Au predeposition the rates were lower by a factor of 10. The quartz-crystal monitor was calibrated by x-ray diffraction measurements of Pb/Ag superlattices (using the method described in Ref. 29) which were confirmed by RHEED intensity oscillation measurements of Au and Ag on Si(111) (Ref. 11) and Pb on Si(111).²⁸

The resistivity was measured during deposition as follows. The 1017-Hz signal from an ac generator was multiplied with the dc signal from the quartz-crystal monitor which is proportional to the mass of the deposited film. The ac-dc product voltage was applied to the Si substrate—which had a typical resistance of about 1 kΩ at 95 K—with a 330 kΩ resistor in series.

This circuit gave a constant current density through the Au film of about 1 μA/nm independent of film thickness d . A signal which is proportional to $R_{\parallel}d$ with $R_{\parallel} = R_s R_f / (R_s + R_f)$, where R_s is the resistance of the substrate, R_f that of the film, was obtained from potential contacts consisting of electrochemically etched W wires pressed against the Si crystal. The signal was measured with a lock-in amplifier and was recorded simultaneously in analog form on a X-Y recorder and in digital form for further evaluation. For each sample typically about 500 measurement points were collected.

The RHEED system was operated at 15–20 keV and consisted of an electrostatically focused electron gun with a 0.3-mm beam-defining aperture, a magnetic focusing lens and sets of magnetic deflection coils for controlling the polar angle of incidence of the electron beam. This angle could be adjusted with an accuracy of ±0.05°. The azimuthal angle was adjusted relative to the Si RHEED pattern with an accuracy of ±1°. The intensity of the specularly reflected beam was measured with a photodiode with a 0.5-mm-diam aperture attached to the fluorescent screen and was recorded during deposition as a function of Pb thickness which was measured simultaneously with the quartz-crystal monitor.

IV. RESULTS AND DATA ANALYSIS

A. Resistivity measurements

Figure 1 shows the result of two typical measurements at 95 K, with the specific resistivity replotted from the

original data in a manner suggested by Eqs. (1) and (2): ρ versus $1/d$ for Eq. (1) [Fig. 1(a)] and $1/(\rho d)$ versus $\ln d$ for Eq. (2) [Fig. 1(b)]. One set of data is from a type-I sample, the other from a type-II sample. The type-I sample shows two linear regions. Apparently the sample undergoes a structural change after reaching a critical thickness of about 1.2 nm and this process is completed at a thickness of about 1.5 nm, that is, within about one monolayer. RHEED indeed clearly shows a dramatic sudden change from a poorly ordered initial layer to a well-ordered epitaxial layer at this thickness.²⁸ The critical thickness does not change with increasing temperature of deposition (and simultaneous resistivity measurement) but the completion of the transition occurs increasingly later, for example, at about 3.0 nm at 200 K. Type-II samples have a completely different thickness dependence of the resistivity. As seen in Fig. 1, the specific resistivity oscillates over a wide coverage range about one linearly rising mean value indicated by the dashed line. This suggests that both type-I and type-II samples can be fitted with straight lines as expressed by Eqs. (1) and (2) in both approximations. These least-

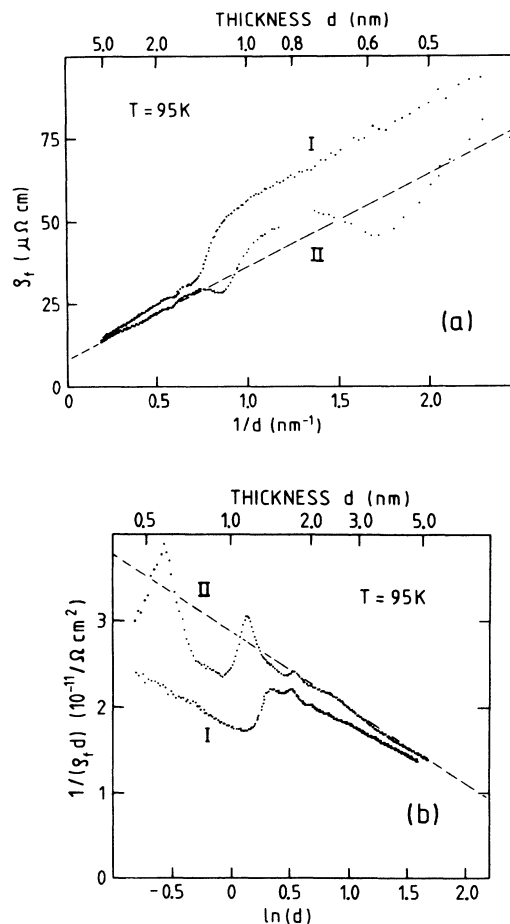


FIG. 1. Specific resistivity of the ultrathin Pb film deposited on a Si(111)-(7×7) surface (type I) and on a Si(111)-Au(6×6) surface (type II) at 95 K, plotted in coordinates (a) according to Eq. (1) and (b) according to Eq. (2).

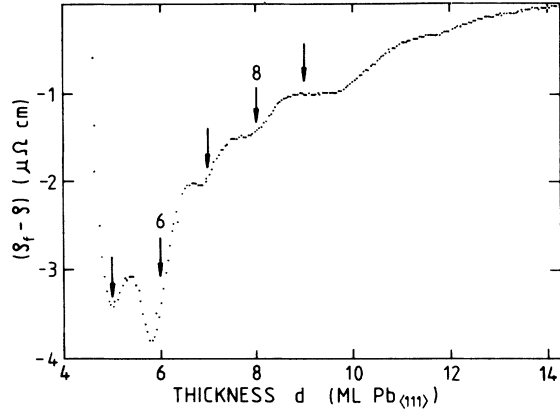


FIG. 2. The difference $\rho_f - \rho$ as a function of thickness of a type-I Pb film at 95 K. ρ is given by Eq. (1) with $\rho_\infty = 6.2 \times 10^{-6} \Omega \text{ cm}$ and $l(1-p) = 17.6 \text{ nm}$.

squares fits give the values $\rho_\infty, (1-p)l$ [from Eq. (1)] and $l, \rho_\infty [(1-p)/(1+p)]l$ [from Eq. (2)] shown in Table I. With the assumption that both equations are satisfactory approximations in the thickness range of interest the results can be combined in order to obtain p , with l from Eq. (2) being used in Eq. (1) and ρ_∞ from Eq. (1) being used in Eq. (2). This leads to the p_1, p_2 values and with Eq. (5) to the p, q values in Table I. It is seen that the p_i values of the type-II layer are significantly larger than those of the type-I layer, which indicates a larger average specularity of the type-II layer. The p, q values derived from the p_i values violate the obvious condition $0 \leq (p, q) \leq 1$, which is not surprising in view of the simplifying assumptions made in deriving Eqs. (1)–(5). Keeping this in mind it appears justified to assign to type-I layers $p = 1.0$ and $q = 0$ while in the type-II layer q has to be 0.26 if p is reduced to 1.0 because $p + q = 2p_1$ [see Eq. (5)]. On the basis of the considerations of Sec. II A it is natural to assign p to the free surface and q to the Pb/Si interface. The interface of the type-I layer thus scatters electrons completely diffusely ($q = 0$) while that of the type-II layer has considerable specularity ($q \approx \frac{1}{4}$). It is interesting to note that the two thickness regions of the type-I sample hardly differ in specularity parameters p, q but only in their bulk properties ρ_∞, l (see Table I).

After having established the average film parameters as a function of thickness the oscillatory part of the resistivity can be extracted now. In type-I samples, that is, Pb

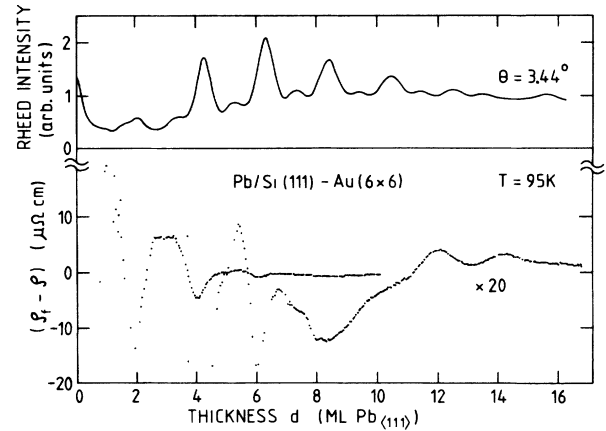


FIG. 3. The difference $\rho_f - \rho$ vs thickness of a type-II Pb film at 95 K. ρ is given by Eq. (1) with $\rho_\infty = 8.2 \times 10^{-6} \Omega \text{ cm}$ and $l(1-p) = 9.4 \text{ nm}$. For comparison the RHEED specular beam intensity oscillations obtained under nearly identical conditions are shown for a glancing angle of incidence of 3.44° .

films on the Si(111)-(7×7) surface, no oscillations are seen during the growth of the first 4 ML ($d \approx 1.2 \text{ nm}$). After the structural transition at this thickness, weak but well-pronounced oscillations with a period of 1 ML occur (Fig. 2). The rapidly changing background in Fig. 2 is caused by the limited validity of Eq. (1) in the vicinity of the transition region. The type-II samples, that is, Pb films grown on the Si(111)-Au(6×6) surface at 95 K, show a quite different behavior as seen in Fig. 3. The resistivity difference curve now shows much stronger oscillations with a period of 2 ML instead of 1 ML and minima at 2, 4, 6, and 8 ML whose depths rapidly decrease with thickness. A second group of oscillations with 2-ML periodicity starts at 9 ML and is most pronounced at 13 ML. The 1-ML periodicity seen in type-I samples (Fig. 2) is hardly visible in type-II samples in the form of weakly pronounced shoulders at 3, 5, and 7 ML.

The differences between the two types of films are even more pronounced at higher temperatures of deposition and measurement as seen in Fig. 4 in which $R_{||}d$ is plotted as a function of d . While in type-I samples the oscillations are absent already at 190 K they are still well pronounced in type-II samples with a 2-ML periodicity at room temperature and, in fact, have been seen even at 360 K. Between 210 K and room temperature actually a third set of oscillations centered at 20 ML is observed in addition to the one centered at 13 ML. These are exactly the thickness values for which the QSE conditions are

TABLE I. Pb film parameters derived from the experimental data of Fig. 1 using Eqs. (1)–(5). For the ρ_∞, l , and p values obtained both Eq. (1) and Eq. (2) are good approximations of the exact Fuchs equation.

Substrate type	Thickness range (nm)	$(1-p)l$ (nm)	ρ_∞ ($\mu\Omega \text{ cm}$)	l (nm)	$\left[\frac{1-p}{1+p} \right] \rho_\infty$ ($\mu\Omega \text{ cm}$)	p_1	p_2	p	q
I	0.4–1.2	2.8	27.6	5.3	17.4	0.46	0.23	1.04	–0.12
I	1.5–5.0	11.5	8.0	20.9	5.0	0.45	0.23	1.01	–0.11
II	0.4–5.0	9.0	8.3	36.8	2.65	0.75	0.51	1.4	0.1

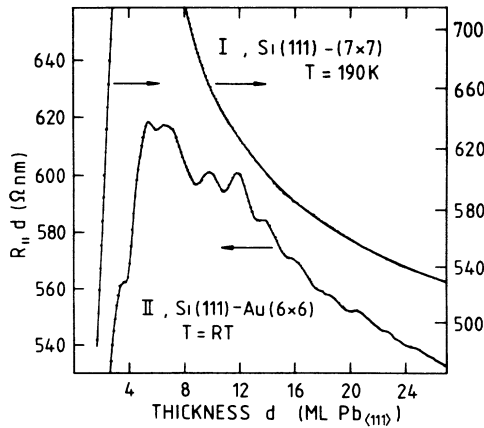


FIG. 4. $R_{\parallel}d = d(R_s R_f)/(R_s + R_f)$ as a function of thickness for a Pb film growing on a Si(111)-(7 \times 7) surface at 190 K and for a Pb film growing on a Si(111)-Au(6 \times 6) surface at room temperature (RT).

best fulfilled in the case of Pb as discussed in Sec.II A. The alternate interpretation of the 2-ML periodicity in terms of double steps can be excluded because (i) there is no reason Pb should grow under otherwise identical conditions on the (7 \times 7) surface monolayer by monolayer, on the Au(6 \times 6) surface double layer by double layer. On thermodynamic grounds the interfacial Au should not diffuse to the growing Pb surface on which it could be adsorbed at steps, thus poisoning them and inducing double step formation. This is supported by experiments which show that in Au-Pb systems the surface is always covered by a Pb layer because of its lower surface energy.³⁰ (ii) Even if Pb should grow on the Si(111)-Au(6 \times 6) surface for some reason with double steps it is inconceivable that the double step structure should be best pronounced at 2, 13, and 20 ML over a wide temperature range, that is, over a wide range of supersaturation during the growth.

B. RHEED specular beam intensity oscillations

The thickness dependence of the specular beam intensity varies strongly with the glancing angle of the incident beam as illustrated in Fig. 5 for Pb growing at 95 K on Si(111) with Au(6 \times 6) structure (type-II samples). Although all curves show a 1-ML periodicity a 2-ML periodicity is superimposed on it at most angles and is most pronounced at about 1.03 $^\circ$, 2.24 $^\circ$, 3.44 $^\circ$, and 4.5 $^\circ$. In contrast to the resistivity QSE oscillations, the 2-ML periodicity is here clearly recognizable over the complete thickness range as best seen at 2.24 $^\circ$ and 3.44 $^\circ$, indicating that some interference condition is fulfilled independent of thickness. Inasmuch as double steps could be excluded as the cause of the 2-ML periodicity in the resistivity oscillations in the previous section the cause of the same periodicity has to be sought here also in the QSE. In order to have constructive interference for even numbers of monolayers independent of film thickness, that is, without the type of modulation (beating) seen in the resistivity QSE oscillations with maxima at 2, 13, and 20 ML, the condition

$$2d_0/(\lambda_z/2) = 2d_0 k_z/\pi = n \quad (n \text{ integer}) \quad (7)$$

must be fulfilled or with Eq. (6) the condition

$$\frac{4d_0}{h} \sqrt{2mE} \left[\sin^2\theta + \frac{V_0}{E} \right]^{1/2} = n. \quad (8)$$

With $E=15000$ eV, a trial value of $V_0=15$ eV, and $d_0=0.286$ nm the θ values shown in Table II for the lowest n values are obtained. The QSE interference model predicts twice as many θ values than were observed. Only the θ values for even n are clearly noticeable in Fig. 5, though an additional enhanced 2-ML periodicity at $\theta \approx 1.55^\circ$ corresponding to $n=5$ is indicated. With increasing n the θ spacings determined by Eq. (8) decrease so that the enhanced 2-ML periodicity may be difficult to see with the θ increments of about 0.17 $^\circ$ in Fig. 5. There is also a systematic discrepancy between the calculated and the experimental θ values which can be eliminated if V_0 is assumed to be θ dependent. The V_0 values obtained

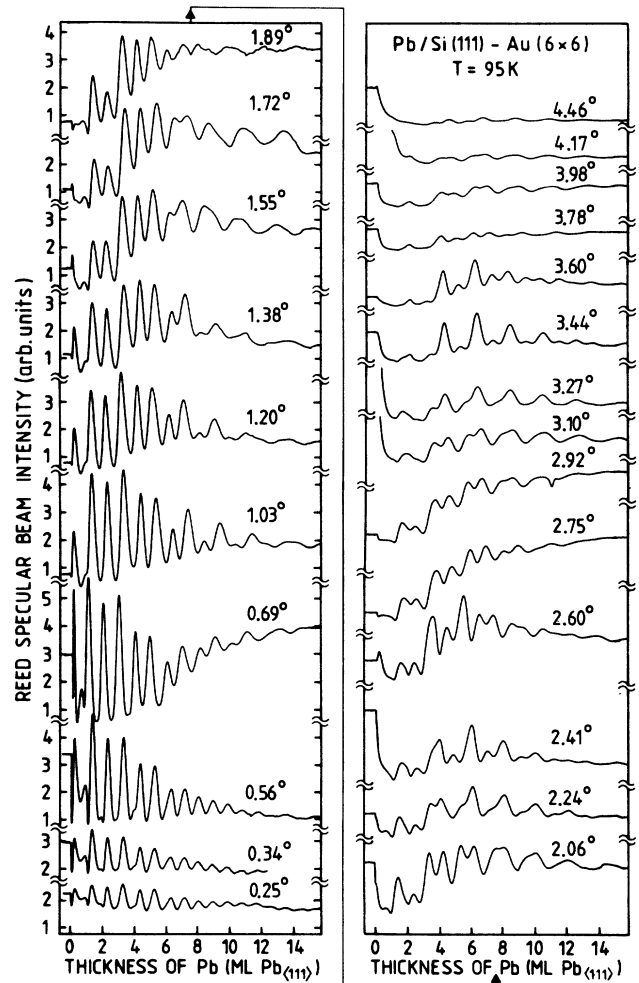


FIG. 5. RHEED specular beam intensity oscillations during the growth of Pb layers on a Si(111)-Au(6 \times 6) surface at 95 K for the indicated polar angles. Azimuth Pb [11 $\bar{2}$], beam energy 15 keV.

TABLE II. Optimum glancing angles of incidence θ for the QSE calculated from Eq. (8) with $V_0 = 15$ eV and from experiment. The experimental θ values give with Eq. (8) the V_0 values shown in the bottom row.

N	3	4	5	6	7	8	9	10
θ_{calc} (deg)		0.85	1.73	2.40	3.00	3.57	4.13	4.67
θ_{expt} (deg)	(0.69)	1.03	(1.55)	2.24		3.44		4.46
V_0 (eV)	(8.1)	13.5	(17.7)	18.3		19.3		23.9

with this assumption from the experimental θ values and Eq. (8) are also listed in Table II. They show a systematic increase of V_0 with θ from 8 to about 19.5 eV, similar to the increase seen in low-energy electron diffraction with increasing energy. The V_0 value for $n = 10$ ($\theta_{\text{expt}} = 4.46^\circ$) is uncertain because the measurements were not continued beyond this angle so that the optimum angle may well be larger and thus V_0 smaller. The normal component of the energy ranges from about 10 to about 115 eV for n increasing from 3 to 10. The larger V_0 values are close to the theoretical values for fast electrons, 18.25–19.4 eV.²⁷ $n = 3$ is possible only for V_0 values below 10.3 eV.

The fact that the QSE features can be seen well over a finite angular range, for example from 3.27° to 3.6° in Fig. 5, and not only at the angle determined by Eq. (8) is in part due to the finite divergence of the beam but probably also in part due to scattering processes in the film. Typical path lengths of electrons reflected at the film-substrate interface are $L = 57$ nm at $\theta = 3.44^\circ$ and $d = 6$ ML, but at 1.03° and 10 ML one has already $L = 318$ nm. Due to this long path considerable inelastic scattering occurs at small angles which reduces coherence and, therefore, the visibility of the QSE. At large angles the total intensity of the specular beam decreases so that the QSE oscillations are more difficult to detect although the oscillations due to the surface interference effects which produce the 1-ML periodicity decrease more strongly with θ . In the intermediate angular range (2° – 4°) the QSE oscillations can be seen best and are well correlated with the resistivity QSE oscillations (Fig. 3).

The main reason for the visibility of the QSE oscillations over a finite angular range, however, is the fact that in the idealized case of a continuously increasing film thickness and in the absence of the periodic surface scattering oscillations QSE oscillations should be visible at any angle of incidence but with a different periodicity. Equation (7) just imposes exact 2-ML periodicity as seen in the experiment. If Eq. (7) were replaced by the condition $d_0/(\lambda_z/2) = n$, the QSE oscillations would have 1-ML periodicity and would coincide with the surface scattering oscillations. They could be extracted from the observed oscillations only if the thickness dependence of the amplitudes of the surface scattering oscillations were known. When the film thickness d changes continuously, d in the QSE condition $d/(\lambda_z/2) = n$ is not limited to $m d_0$ ($m = 1, 2, \dots$) so that QSE oscillations can occur for any θ but their periods will not be multiples of a ML. If they were superimposed on surface scattering oscillations then these would be modulated and distorted by the QSE

periodicity which would be difficult to detect. The modulation is clearly visible only if the QSE periodicity is close to a multiple of the surface scattering periodicity.

As mentioned in Sec. IV A the QSE oscillations of the resistivity become more pronounced with increasing terrace width on the film surface, that is, with increasing temperature. This is also well reflected in the QSE oscillations at higher temperature as indicated in Fig. 6 for the room-temperature range. While at the small glancing angle ($\theta = 0.46^\circ$), far from the lowest QSE condition ($n = 3$, $\theta = 0.7^\circ$), the oscillations due to the monolayer-by-monolayer growth are clearly visible, only the oscillations with 2-ML periodicity attributed to the QSE effect are seen at $\theta \approx 0.7^\circ$ where they are still weakly pronounced at 95 K (Fig. 5). Similar to the resistivity oscil-

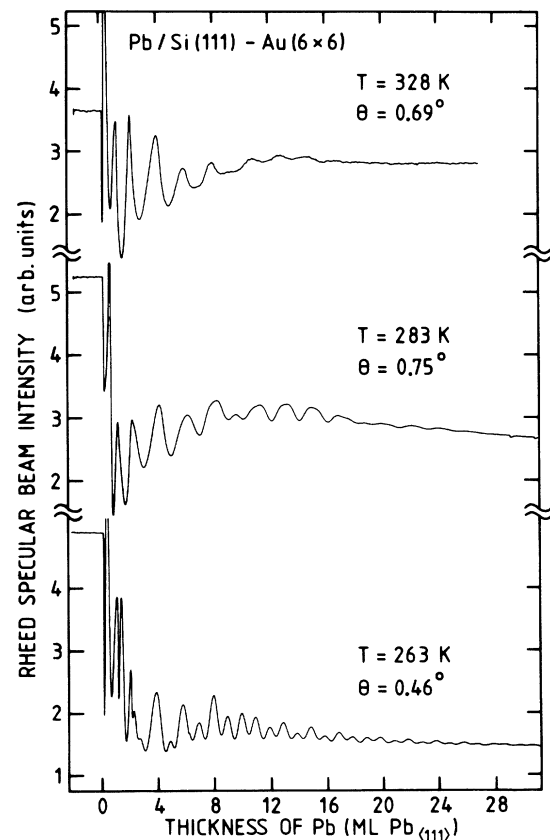


FIG. 6. RHEED specular beam intensity oscillations during the growth of Pb layers on a Si(111)-Au(6×6) surface at different temperatures. Azimuth Pb[112], beam energy 20 keV.

lations, the type-I samples [Pb on Si(111)-(7×7)] showed predominantly oscillations with 1-ML periodicity whose amplitude decreased rapidly with increasing temperature. Above 150 K only some irregular intensity variations with thickness were observed. These differences between the two types of samples are due to differences in film growth caused by the difference between the two substrate surfaces.²⁸ The overall RHEED patterns (length and width of diffraction streaks) clearly show that the Pb films on the Si(111)-Au(6×6) surface are more perfect than those on the Si(111)-(7×7) surface.

V. DISCUSSION AND SUMMARY

For the QSE of the resistivity of a thin film to occur two conditions must be fulfilled: (i) the thickness variations Δd must be small compared to the Fermi wavelength, which for metals usually is less than 1 nm, e.g., for Pb 0.366 nm; and (ii) both surfaces must have sufficient specular reflectivity. Condition (i) requires that the film grows monolayer by monolayer, with terrace widths of the order of the mean free path of the conduction electrons or larger. Then condition (ii) is fulfilled simultaneously for the free surface of the film but not necessarily for the film-substrate interface, even if it is atomically flat for hundreds of nm. There must be in addition a sufficiently high potential step and/or no allowed states at the film's Fermi energy in the substrate and no diffuse scattering centers at the interface. The symmetric situation assumed in all QSE calculations is certainly not fulfilled in most experiments, including the present one. Neither does the film thickness increase continuously as assumed in QSE theory but rather in steps of one monolayer height.

A low specular reflectivity p of one interface appears in the average resistivity versus thickness relations Eqs. (1) and (2) as a lower average p value and reduces the resistivity oscillations produced by p variations at the free surface due to the varying density of steps which cause diffuse scattering. For the QSE a small p at the interface is even more serious so that it is unobservable in the Pb films on the Si(111)-(7×7) surface (Fig. 2). The cause of the small p at this interface—small potential step or diffuse scattering—is unknown at present, as is the cause of the larger p at the Pb-Si(111)-Au(6×6) interface. Films with this interface not only have a larger p but are more perfect and have larger terrace widths so that the resistivity oscillations are dominated by the QSE (Fig. 3). The differences between the two types of film are even more evident at higher temperatures (Fig. 4).

As the film thickness changes in steps of 1 ML height and as the Fermi wavelength λ_F is in general not com-

mensurate with d_0 the signature of the QSE is not a monotonic oscillation of the resistivity with thickness but rather a strongly modulated oscillation with maxima for $md_0 \approx n\lambda_F/2$, as observed in this study. If the oscillation were monotonic it could also be caused in the present case by double-layer-by-double-layer growth due to scattering by the double steps.

The exclusion of double steps on the basis of the modulation of the resistivity oscillations requires also an explanation of the 2-ML periodicity of the RHEED specular beam intensity without double step. Such an explanation is provided again by the QSE which has been reported before for a fundamentally similar situation, low-energy electron reflection at normal incidence.⁶ The QSE condition Eq. (6) together with the condition of unmodulated oscillations leads via Eqs. (7) and (8) to the prediction of optimum angles for the observation of the RHEED QSE which agree well with experiment provided the inner potential is assumed to depend upon normal energy similar to the situation in LEED.

QSE oscillations should always be present in RHEED in the monolayer-by-monolayer growth of films which differ sufficiently from the substrate that standing waves can build up in the films. They are superimposed on the intensity oscillations with 1-ML periodicity caused by the periodic reproduction of the surface microstructure. Indications of such a modulation have actually been seen in the epitaxy of various metals on a W(110) surface.⁹

In conclusion, QSE oscillations have been seen both in the resistivity and in the RHEED specular beam intensity of Pb films during the growth on Si(111) surfaces. These QSE oscillations are superimposed on the oscillations caused by the scattering of the electrons at the growing film surface. Their separation requires favorable growth conditions which were obtained by surface modification of the Si(111) surface by Au. The stringent requirements for the occurrence of the QSE in the resistivity of metal films make it likely that it can be observed only in carefully prepared epitaxial films. In the RHEED specular beam intensity, however, the QSE should be common but it is more difficult to separate it from the surface-induced oscillations.

ACKNOWLEDGMENTS

This work was supported by the Volkswagen Foundation (Hannover, Germany) and in part by the Polish Academy of Sciences Lublin Physics Research Project No. CPBP-1.08.C-1.3. One of the authors (M.J.) wishes to thank the Alexander von Humboldt Foundation (Bonn, Germany) for financial support which allowed him to do this work in Clausthal.

¹K. F. Schulte, Surf. Sci. **55**, 427 (1976); Phys. Status Solidi B **79**, 149, K5 (1977).

²P. J. Feibelman, Phys. Rev. B **27**, 1991 (1983); P. J. Feibelman and D. R. Hamann, *ibid.* **29**, 6463 (1984).

³S. Ciraci and I. P. Batra, Phys. Rev. B **33**, 4294 (1986); I. P. Batra, S. Ciraci, G. P. Srivastava, J. S. Nelson, and C. Y. Fong,

ibid. **34**, 8246 (1986).

⁴J. P. Rogers III, P. H. Cutler, T. E. Feuchtwang, and A. A. Lucas, Surf. Sci. **141**, 61 (1984); **181**, 436 (1987).

⁵R. C. Jaklevic, J. Lambe, M. Mikkor, and W. C. Vassell, Phys. Rev. Lett. **26**, 88 (1971); R. C. Jaklevic and J. Lambe, Phys. Rev. B **12**, 4146 (1975).

- ⁶B. T. Jonker, N. C. Bartelt, and R. L. Park, *Surf. Sci.* **127**, 183 (1983); B. T. Jonker and R. L. Park, *ibid.* **146**, 93 (1984); **146**, 511 (1984); *Solid State Commun.* **51**, 871 (1984); H. Iwasaki, B. T. Jonker, and R. L. Park, *Phys. Rev. B* **32**, 643 (1985).
- ⁷E. Bauer, *Z. Kristallogr.* **110**, 372 (1958); E. Bauer and H. Poppa, *Thin Solid Films* **12**, 167 (1972); E. Bauer and J. H. van der Merwe, *Phys. Rev. B* **33**, 3657 (1986).
- ⁸E. Bauer, H. Poppa, G. Todd, and F. Bonczek, *J. Appl. Phys.* **45**, 5164 (1974); E. Bauer, H. Poppa, G. Todd, and P. R. Davis, *ibid.* **48**, 3773 (1977).
- ⁹G. Lilienkamp, C. Koziol, and E. Bauer, in *RHEED and Reflection Electron Imaging of Surfaces*, edited by P. K. Larsen (Plenum, New York, in press).
- ¹⁰G. Fischer and H. Hoffmann, *Z. Phys. B* **39**, 287 (1980); G. Fischer, H. Hoffmann, and J. Vancea, *Phys. Rev. B* **22**, 6065 (1980).
- ¹¹M. Jałochowski and E. Bauer, *Phys. Rev. B* **37**, 8622 (1988).
- ¹²K. Fuchs, *Proc. Cambridge Philos. Soc.* **34**, 100 (1938).
- ¹³E. H. Sondheimer, *Adv. Phys.* **1**, 1 (1952).
- ¹⁴K. L. Chopra, *Thin Film Phenomena* (McGraw-Hill, New York, 1969), pp. 344ff.
- ¹⁵J. R. Sambles, K. C. Elsom, and D. J. Jarvis, *Philos. Trans. R. Soc. London, Ser. A* **304**, 365 (1982); J. R. Sambles, *Thin Solid Films* **106**, 321 (1983).
- ¹⁶C. R. Tessier and A. J. Tosser, *Size Effects in Thin Films* (Elsevier, Amsterdam, 1982).
- ¹⁷H. Hoffmann, in *Advances in Solid State Physics*, edited by P. Grosse (Vieweg, Braunschweig, 1982), Vol. 22, p. 255; G. Reiss, J. Vancea, and H. Hoffmann, *Phys. Rev. Lett.* **56**, 2100 (1986).
- ¹⁸H. J. Juretschke, *Surf. Sci.* **2**, 40 (1964); *J. Appl. Phys.* **37**, 435 (1966); M. S. P. Lucas, *ibid.* **36**, 1632 (1965).
- ¹⁹G. Govindaraj and V. Devanathan, *Phys. Rev. B* **34**, 5904 (1986).
- ²⁰J. R. Anderson and A. V. Gould, *Phys. Rev.* **A139**, 1459 (1965).
- ²¹A. A. Neto and L. G. Ferreira, *Phys. Rev. B* **14**, 4390 (1976).
- ²²K. Horn, B. Reihl, A. Zartner, D. E. Eastman, K. Hermann, and J. Noffke, *Phys. Rev. B* **30**, 1711 (1984).
- ²³J. R. Chelikowsky and M. L. Cohen, *Phys. Rev. B* **14**, 556 (1976).
- ²⁴L. J. Brillson, *Surf. Sci. Rep.* **2**, 123 (1982).
- ²⁵C. S. Lent and P. I. Cohen, *Phys. Rev. B* **33**, 8329 (1986); P. I. Cohen, P. R. Pukite, J. M. van Hove, and C. S. Lent, *J. Vac. Sci. Technol. A* **4**, 1251 (1986), and references therein.
- ²⁶S. Clarke and D. D. Vvedensky, *Phys. Rev. Lett.* **58**, 2235 (1987); *Appl. Phys. Lett.* **51**, 340 (1987).
- ²⁷G. Radi, *Acta Crystallogr., Sect. A* **26**, 41 (1970).
- ²⁸M. Jałochowski and E. Bauer, *J. Appl. Phys.* **63**, 4501 (1988).
- ²⁹M. Jałochowski and P. Mikołajczak, *J. Phys. F* **13**, 1973 (1983).
- ³⁰A. K. Green, S. Prigge, and E. Bauer, *Thin Solid Films* **52**, 163 (1978), and references therein.